On the Unusual Properties of Halogen Bonds: A Detailed ab Initio Study of $X_2-(H_2O)_{1-5}$ clusters (X = Cl and Br)

Margarita I. Bernal-Uruchurtu* and Ramón Hernández-Lamoneda

Centro de Investigaciones Químicas, Universidad Autónoma del Estado de Morelos, Cuernavaca, 62209, México

Kenneth C. Janda

Department of Chemistry, University of California, Irvine, California 92697

Received: January 17, 2009; Revised Manuscript Received: March 12, 2009

Halogen bonds have received a great deal of attention in recent years. Their properties, sometimes paralleled with those of hydrogen bonds, have not yet been fully understood. In this work, we investigate the nature of the intermolecular interactions between Cl_2 and Br_2 with water. Our analysis of several features of MP2/aug-cc-pVDZ-optimized stable clusters with different number and arrangement of water molecules shows that two different kinds of halogen−water coordination patterns are involved in the stability and properties found for these systems: halogen bonds (X−X···O) and halogen−hydrogen interactions, (X−X···H−O−H). Both types of interactions result in a large polarization of the halogen molecule, which leads to important cooperative effects on these structures. Although the general structural aspects of these clusters can be understood in terms of dipole−quadrupole forces at long range, where it is the dominant term, the SAPT analysis shows that factors such as polarization of π densities and dispersion become increasingly important close to equilibrium. In particular, we show that the halogen−hydrogen interactions are weaker than halogen−oxygen interactions mainly due to the electrostatic and dispersion forces. We also calculate vibrational and electronic shifts that should be helpful for the interpretation of experimental results and for investigating the microsolvation phenomena for halogens in an aqueous environment.

Introduction

Halogen molecules provided one of the early model systems for understanding solvent effects on molecular spectra because they are apparently simple molecules whose spectra shift substantially in different solvents. For instance, even though I_2 has no dipole moment, its color changes completely in polar solvents. In a noninteractive solvent, such as hexane, a dilute iodine solution is violet in color. In a solvent of higher polarity, such as dichloromethane, the solution is a rose color. An aqueous solution of iodine is yellow. Clearly, the iodine spectrum is very sensitive to the local environment. The spectra of chlorine and bromine are somewhat less sensitive to the details of the solvent. For instance, the valence excitation band of iodine is blue shifted by 2820 cm^{-1} in aqueous solution relative to the gas phase.[1] For bromine[2] the comparable blue shift is only 1750 cm^{-1}, and for chlorine it is 550 cm^{-1}.[3]

From 1948 to 1955 this model system received considerable attention since it appeared to be one for which a detailed analysis of both the nearest neighbor and continuum effects might be possible.[4−6] However, the tools available at the time did not make it possible to quantitatively model the nearest neighbor effects, and the continuum solvent models were not completely satisfying. For instance, the solvation model that consists of a chromophore within a cavity of a dielectric predicts that the solvent shift should be proportional to the square of the transition moment.[7,8] This was not found to be the case, in general. Therefore, for many years the halogens fell out of favor as a model system for understanding solvent effects on spectra. There have been few recent papers on this subject.[9]

Thirty years ago, the halogens became a popular model system for studying nearest neighbor effects on spectroscopy with the advent of molecular beam studies of dimers and small clusters.[10,11] The expectation was that noble-gas interactions with halogens would provide a model system that could provide a framework for understanding systems that are more complicated. Again, however, this apparently simple model system proved to be more complicated than expected.[12−15] For instance, it took almost 30 years to work out the details of how different the spectroscopy is depending on whether the noble-gas atom is on the side of the halogen to form a T-shaped complex or on the end to form a linear complex.[16,17] For the T-shaped complex the noble-gas atom induces a relatively small spectral shift of the halogen valence electronic transitions of the halogens, from ~3 cm^{-1} for helium to ~20 cm^{-1} for Ar.[18] The spectra exhibit well-defined rotational substructure that can be used to determine the bond lengths of the complexes. Homogeneous broadening and pump−probe spectroscopy could be employed to characterize vibrational energy transfer from the halogen stretching vibration to the dissociative van der Waals coordinate. A rich literature has grown around the dynamics of this phenomenon.[19]

Linear noble-gas−halogen dimers have proved to be more difficult to study than the T-shaped ones even though they were the first to be observed. Because the ground-state potential-energy well of the linear isomer lies below the repulsive portion of the excited-state surface, the linear species have predominantly continuum spectra in the valence excitation region. Burke and Klemperer were the first to quantitatively measure this

* To whom correspondence should be addressed. E-mail: mabel@uaem.mx.

10.1021/jp900490p CCC: $40.75
Published on Web 04/15/2009

continuum,[20] and then Darr, Glennon, and Loomis were able to measure specific excitation thresholds that resulted in direct measure of the bond energies for these species.[21] Recently, Pio et al. were able to measure excitation spectra for He−, Ne−, and Ar−Br_2 that helped illustrate how the continuum spectra depend on the details of the nearest neighbor interactions.[19] Even for the noble-gas−halogen system, however, the details of how the nearest neighbor interactions combine with continuum effects to yield condensed phase spectra have yet to be completely understood.

As may be expected, the interaction between halogen and water molecules is considerably stronger than between halogens and noble gases. Although no valence electronic excitation spectra have yet been reported for this system, the group of Legon obtained the microwave spectra for several of the H_2O-X_2 species.[22−26] For instance, in the case of H_2O-Br_2 the bonding can be characterized as the oxygen lone pair electrons donating to the σ^* orbital in Br_2 to form a strong halogen bond. The resulting bond length is 0.3 Å less than the sum of the O and Br van der Waals radii, and the well depth is ∼2/3 that of the water dimer. As for the linear noble-gas−halogen dimers, valence electronic excitation of H_2O-X_2 would leave the dimer on a repulsive portion of the weak bonding coordinate, resulting in a substantial blue shift of the spectrum. Indeed, our first estimate of the dimer blue shift is that it is greater than the entire solvent shift for Br_2 in aqueous solution.[27]

The spectroscopy of Br_2 and I_2 have also been studied in clathrate hydrate solids.[1,2,28] Clathrate hydrates consist of a solid lattice in which the water molecules form different sized cages. For instance, a 28 water molecule cage that has 12 pentagonal faces and 4 hexagonal faces with an oxygen atom at each vertex and a hydrogen atom along each edge is referred to as a $5^{12}6^4$ clathrate hydrate cage. 5^{12} and $5^{12}6^4$ cages combine in a 2:1 ratio to form a solid lattice, slightly less stable than hexagonal ice but more stable if each of the large cages contains a Br_2 molecule. The valence electronic spectrum of Br_2 in such a cage is blue shifted from the gas phase by 440 cm^{-1}, 1320 cm^{-1} less than in aqueous solution. The initial explanation for this result is that all of the oxygen lone electron pairs of water molecules in a clathrate hydrate cage are involved in hydrogen bonding and thus unavailable to interact strongly with the Br_2 molecule.

The detailed experimental work of Legon's group on the interaction of dihalogens with different Lewis bases in the gas phase has been used to emphasize the close similarities between halogen bonds (XB) and hydrogen bonds (HB).[24−26,29] Their conclusions are sustained by a large body of rotational experiments on 1:1 complexes. Their work confirms that the equilibrium angular geometry of a halogen-bound complex, B···X−Y, can be predicted by assuming that the internuclear axis of the dihalogen molecule (X−Y) lies along the axis of a nonbonding electron pair carried by the acceptor atom Z of B ($Z\cdots^{\delta+}X-Y^{\delta-}$). This argument has been used to explain the reasons why the significant nonlinearity of hydrogen bonds is absent in halogen bonds. An argument along the same line has been developed by other groups.[30−33]

In a recent work, Pathak et al.[34] reported several stable structures for halogen−water clusters up to eight water molecules whose optimized geometries were obtained using DFT methodologies. An interesting finding of their work is that the most stable structures of chlorine, bromine, and iodine with 1−6 water molecules are quite similar except for the case with two water molecules. Their work, aimed at understanding the hydration process for these species, focused on the effects of polarizability. They did not comment on the other intermolecular forces. In this paper we work toward a more complete understanding of the interactions between halogen and water molecules by studying the electronic structure of $Cl_2-(H_2O)_n$ and $Br_2-(H_2O)_n$ clusters.

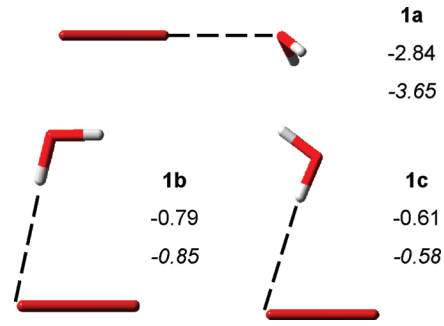

Figure 1. Optimized structures for the X_2-H_2O complex at the MP2/aug-cc-pVDZ level. Thick dashed lines show the nonbonded interaction between the halogen molecule and water. Full counterpoise BSSE-corrected MP2/aVDZ interaction energies for Cl_2 and Br_2 (in italics) structures are shown in kcal/mol. The corresponding distances for the complexes are presented in Table 1.

Methodology

Geometry optimizations for the $X_2-(H_2O)_n$ clusters were performed at the MP2/aug-cc-pVDZ level using the Gaussian set of programs[35] starting from several different initial geometries. Although this basis results in sizable basis set superposition errors, it yields geometric minima in good agreement with those from experimental work and larger basis sets as discussed in our previous work.[27] We correct the BSSE error on the interaction energies using the full-counterpoise correction. A harmonic frequency analysis was performed to confirm that each stationary point corresponds to a local minimum in the potential-energy surface (PES). We used Mulliken and natural bond orbital (NBO) analyses for the charge distribution analysis and the charge transfer calculations in the clusters. For the smallest clusters, a symmetry-adapted perturbation theory (SAPT) analysis of the interaction energy was also obtained with the aug-cc-pVTZ basis. Finally, we calculated vertical B ⇐ X transition energies for the clusters using the RMP2 and RCCSD(T) methods as implemented in Molpro 2006.1[36] Many-body terms were calculated within the noncanonical scheme that leads to convergent results for fully relaxed systems.[37,38] It is referred to as the noncanonical scheme because the relaxation energy of the monomers is included as a zero-order term on the expansion, in contrast to other schemes in which the deformation of the monomers is implicitly considered in the two-body term. Thus

$$E^{\mathrm{int}}_{i,j,\ldots,n} = \sum V_{ij} + \sum \delta_i + \eta_3 + \ldots + \eta_n \qquad (1)$$

where δ_i corresponds to the relaxation energy of the monomers calculated as $\delta_i = E_i - E_0$ and the two-body terms as $V_{ij} = E_{ij} - (E_i - E_j)$. Larger contributions, for example, the three-body nonadditivities, are obtained in the usual form as

$$\eta_3 = E^{\mathrm{int}}_{ijk} - \sum_{ij} V_{ij} - \sum \delta_i \qquad (2)$$

All calculations of nonadditivities were done at the MP2 level and with full counterpoise; i.e., the energy of each subsystem ($\langle i\rangle$, $\langle ij\rangle$ or $\langle i, j, \ldots\rangle$) at the cluster geometry is evaluated in the full basis of the complete cluster ($\langle i, j, \ldots, n\rangle$) considered. This counterpoise correction has proven to be necessary for a proper description of nonadditivities and in a critical manner when

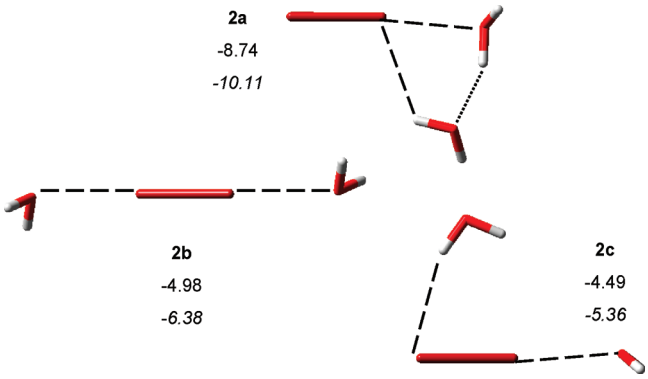

Figure 2. Optimized structures for the $X_2-(H_2O)_2$ complex at the MP2/aug-cc-pVDZ level. Thick dashed lines show the nonbonded interaction between the halogen molecule and water, and thin lines show the hydrogen bonds formed between water molecules. Full counterpoise BSSE-corrected MP2/aVDZ interaction energies for Cl_2 and Br_2 (in italics) structures are shown in kcal/mol. The corresponding distances for these complexes are presented in Table 1.

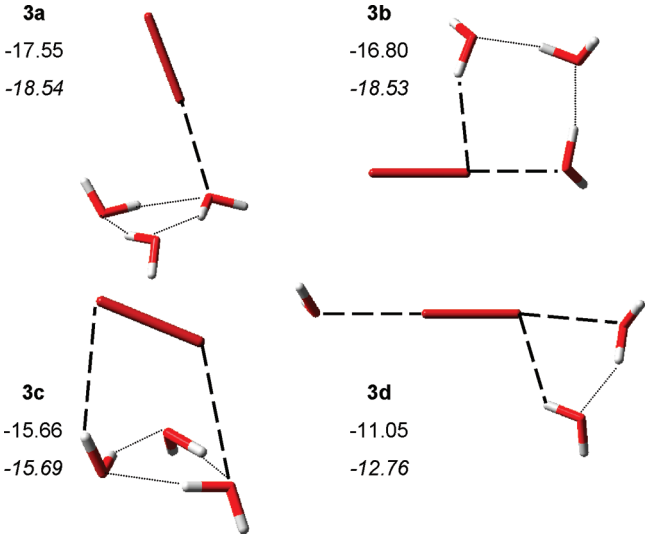

Figure 3. Optimized structures for the $X_2-(H_2O)_3$ complex at the MP2/aug-cc-pVDZ level. Thick dashed lines show the nonbonded interaction between the halogen molecule and water, and thin lines show the hydrogen bonds formed between water molecules. Full counterpoise BSSE-corrected MP2/aVDZ interaction energies for Cl_2 and Br_2 (in italics) structures are shown in kcal/mol. The corresponding distances for these complexes are presented in Table 1.

correlation energy is included. In particular, the use of a limited basis set, such as the one employed here, emphasizes the need of its use.

Results

I. Structure and Relative Stabilities of Stable $X_2-(H_2O)_{1-5}$ Clusters. ***A. Stable Structures.*** In Figures 1−5 we present the most stable structure and several low-lying isomers found for the $X_2-(H_2O)_{1-5}$ clusters along with the corresponding BSSE-corrected interaction energies. Although the search for minima was not exhaustive, we started from a wide variety of initial geometries to improve the chance of finding unexpected minima. For each value of n, we show examples of isomers that are qualitatively different from each other. In some cases, more than one minimum was found with a similar overall appearance. In those cases, only the lowest energy conformer is shown. Table 1 gives selected geometrical parameters; Table 2 gives the partial charge differences of the halogen atoms in the molecule and

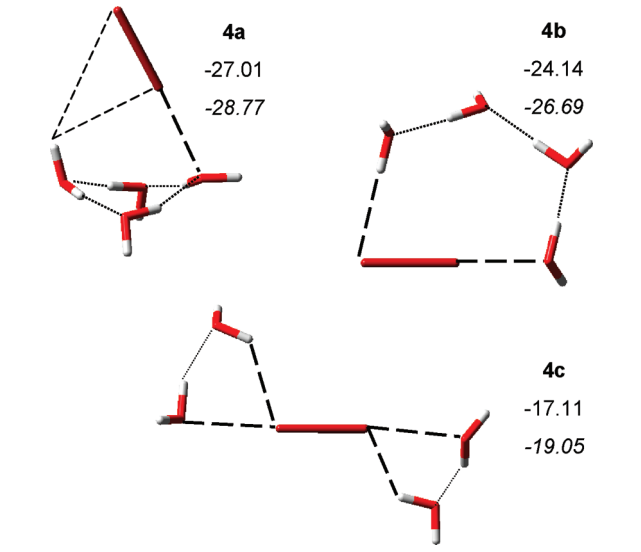

Figure 4. Optimized structures for the $X_2-(H_2O)_4$ complex at the MP2/aug-cc-pVDZ level. Thick dashed lines show the nonbonded interaction between the halogen molecule and water, and thin lines show the hydrogen bonds formed between water molecules. Full counterpoise BSSE-corrected MP2/aVDZ interaction energies for Cl_2 and Br_2 (in italics) structures are shown in kcal/mol. The corresponding distances for these complexes are presented in Table 1.

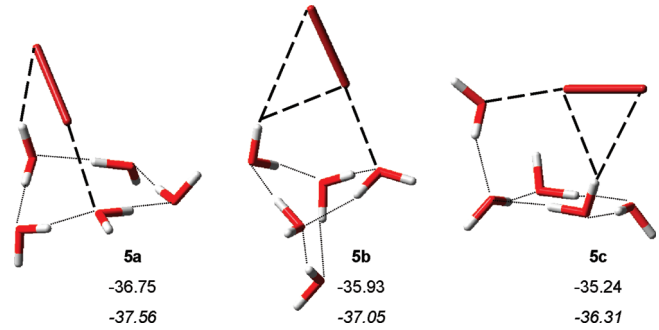

Figure 5. Optimized structures for the $X_2-(H_2O)_5$ complex at the MP2/aug-cc-pVDZ level. Thick dashed lines show the nonbonded interaction between the halogen molecule and water, and thin lines show the hydrogen bonds formed between water molecules. Full counterpoise BSSE-corrected MP2/aVDZ interaction energies for Cl_2 and Br_2 (in italics) structures are shown in kcal/mol. The corresponding distances for these complexes are presented in Table 1.

the charge transfer calculated for selected clusters; Table 3 gives the many-body analysis for two selected cases of the $X_2-(H_2O)_2$ and $X_2-(H_2O)_3$ clusters that will help to illustrate the relative importance of the several concurring forces in these clusters. The complete analysis for all the studied clusters is provided as Supporting Information.

For the 1:1 complex, three stationary points were found: the halogen-bonded (XB) structure **1a** and two different H-bonded geometries **1b** and **1c**. Qualitatively, the halogen-bonded structure appears to have the oxygen lone electron pair donated to the halogen σ^* LUMO, as originally discussed by Legon. The hydrogen bonds involve interaction of the electropositive hydrogen atom with the halogen π^* HOMO. These preferred orientations are also consistent with the strong dipole−quadrupole interactions to be expected for these types of monomers, and this point of view is further analyzed below. Note that although the hydrogen-bond lengths are less than the sum of the van der Waals radii, 3.04 Å, the bond energies are much smaller than the halogen-bonded one and much smaller than for hydrogen bonding between water molecules. To avoid confusion, for the

TABLE 1: Selected Structural Parameters of the Optimized Stable Structures Found for $X_2-(H_2O)_n$[a]

		X = Cl	X = Br				
cluster	structure	r(Cl−Cl)	r(Cl···O) (θ, Cl−Cl−O)	r(Cl···H) (θ, Cl−Cl−H)	r(Br−Br)	r(Br···O) (θ, Br−Br−O)	r(Br···H) (θ, Br−Br−H)
X_2-H_2O	**1a**	2.050	2.755 *(180)*		2.338	2.769 *(180)*	
	1b	2.040		2.614 *(175)*	2.291		2.705 *(174)*
	1c	2.039		2.616 *(163)*	2.325		2.721 *(171)*
$X_2-(H_2O)_2$	**2a**	2.058	2.672 *(175)*	2.741 *(128)*	2.351	2.674 *(175)*	2.880 *(124)*
	2b	2.057	2.831 *(179)*		2.347	2.876 *(179)*	
	2c	2.052	2.714 *(175)*	2.735 *(153)*	2.324	2.749 *(178)*	2.796 *(156)*
$X_2-(H_2O)_3$	**3a**	2.052	2.715 *(176)*		2.344	2.726 *(175)*	
	3b	2.065	2.582 *(177)*	2.435 *(162)*	2.364	2.568 *(173)*	2.570 *(155)*
	3c	2.040	3.185 *(126)*	2.938 *(132)*	2.329	3.330 *(121)*	3.000 *(136)*
	3d	2.061	2.783 *(173)*2.815 *(179)*	2.619 *(135)*	2.352	2.802 *(173)*2.875 *(179)*	2.741 *(134)*
$X_2-(H_2O)_4$	**4a**	2.052	2.735 *(175)*	3.301 *(104)* 3.396 *(135)*	2.383	2.749 *(175)*	3.319 (109) 4.255 (142)
	4b	2.079	2.489 *(179)*	2.409 *(176)*	2.358	2.470 *(179)*	2.255 *(176)*
	4c	2.066	2.758 *(174)* 2.768 *(173)*	2.669 *(132)* 2.655 *(133)*	2.344	2.793 *(174)* 2.806 *(173)*	2.765 *(132)* 2.756 *(133)*
$X_2-(H_2O)_5$	**5a**	2.051	2.724 *(164)*	2.810 *(145)*	2.344	2.722 *(166)*	3.024 *(150)*
	5b	2.054	2.707 *(176)*	2.860 *(128)* 3.651 *(162)*	2.347	2.718 *(177)*	2.941 *(130)* 3.996 *(163)*
	5c	2.054	2.687 *(172)*	2.782 *(136)* 2.980 *(112)*	2.350	2.675 *(172)*	2.926 *(141)* 3.045 *(114)*

[a] Distances are in Angstroms and angles, in parentheses, in degrees. Bond distances for Cl_2 and Br_2 at this level (MP2/aVDZ) are 2.039 and 2.328 Å, respectively.

TABLE 2: Halogen Molecule Polarization in the $X_2-(H_2O)_n$ clusters (δq) and Total Charge Per Molecule of Some Selected Clusters[a]

structure	halogen	δq	X_2	W1	W2	W3	W4	W5
1a	Cl_2	0.055	−0.018	0.018				
	Br_2	0.078	−0.027	0.027				
1b	Cl_2	0.026	0.009	−0.009				
	Br_2	0.029	0.011	−0.011				
2a	Cl_2	0.062	−0.027	0.011	0.016			
	Br_2	0.095	−0.043	0.025	0.018			
2c	Cl_2	0.057	−0.012	0.020	−0.008			
	Br_2	0.082	−0.018	0.028	−0.009			
3a	Cl_2	0.053	−0.018	0.000	0.006	0.012		
	Br_2	0.080	−0.030	0.003	0.012	0.014		
3b	Cl_2	0.083	−0.029	0.013	0.010	0.006		
	Br_2	0.132	−0.054	0.032	0.009	0.013		
4a	Cl_2	0.056	−0.019	0.007	−0.001	0.008	0.005	
	Br_2	0.082	−0.031	0.010	0.000	0.012	0.008	
4b	Cl_2	0.137	−0.049	0.028	0.013	0.004	0.003	
	Br_2	0.055	−0.079	0.054	0.008	0.005	0.011	
5a	Cl_2	0.065	−0.010	0.004	0.000	0.006	−0.004	0.004
	Br_2	0.096	−0.023	0.005	0.006	−0.003	0.008	0.007
5b	Cl_2	0.052	−0.018	0.000	−0.010	0.005	0.012	0.010
	Br_2	0.101	−0.034	0.009	−0.003	0.020	−0.013	0.022

[a] Values were obtained using NBO charges. All reported values are in au. For cases with several water molecules in the cluster, W1 refers to the XB water molecule and W2 to the XH bound (if any).

larger clusters only bonds between water molecules will be referred to as hydrogen bonds, HB, and the halogen−hydrogen bonds will be denoted as XH bonds. This differentiation will be supported by a SAPT analysis presented below. It is also interesting to note that for structure **1a** there is negligible charge transfer from the water to the halogen, 0.02 au for Cl_2 and 0.03 au for Br_2, but that the halogen molecule is somewhat polarized, $\delta q = 0.1$ au for Cl_2 and 0.14 au for Br_2, with the negative charge on the outer halogen atom in each case. In the XH-bound structures, the charge transfer is even smaller than for XB, but it occurs in an inverse sense than for the latter.

The stable structures found for $X_2-(H_2O)_2$ start to illustrate the cooperative effects between hydrogen bonding, halogen bonding, and XH bonding. In this sense, the most stable geometry, structure **2a**, has a surprising coordination motif in which one of the halogen atoms is simultaneously engaged in both XB and XH bonds with the two ends of a water dimer. The charge analysis of structure **2a** reveals two interesting results. First, although there is now both halogen bonding and hydrogen bonding in the same structure, the charge transfer is only slightly larger than for structure **1a** with only halogen bonding, 0.03 for Cl_2 and 0.04 for Br_2. Second, the XH bond is formally between two positively charged atoms: $H^{\delta+}\cdots{}^{\delta+}X$. Wang et al.[39] describe this case as an "unusual halogen-bonded complex", but Politzer et al. point out that the halogen atom has a negative electrostatic potential around its axis due to the π and π^* electrons,[40] and as previously mentioned, dipole−quadrupole interactions favor this type of arrangement.

In structures **2b** and **2c** each halogen atom coordinates to a different water molecule: in structure **2b** two XB bonds are formed, and in **2c** there is one XB and one XH bond. In each case, the XB bonds are along the halogen axis and the XH bonds are nearly perpendicular to the halogen axis. Note that although structure **2b** can be considered as a double **1a**, the length of the XB in it is ∼0.1 Å larger than for structure **1a**, reflecting its reduced stability. On the other hand, structure **2c** may be thought as **1a** + **1b** but with shorter intermolecular distances. Charge transfer in this structure is very close to that for structure **2a**. The many-body analysis for these clusters, see Table 3, confirms the contribution of halogen polarization and charge transfer to the observed stability. Surprisingly, for **2a** and **2b** the two-body halogen−water terms are more attractive than for the corre-

TABLE 3: Many-Body Analysis of the Interaction Energies for Selected Stable $X_2-(H_2O)_2$ and $X_2-(H_2O)_3$ Clusters[a]

cluster					X = Cl					X = Br				
					E_{int}	$\Sigma\delta_i$	ΣV_{ij}	η_{ijk}	η_{ijkl}	E_{int}	$\Sigma\delta_i$	ΣV_{ij}	η_{ijk}	η_{ijkl}
2a						**0.16**					**0.21**			
	X_2	W1			−2.45					−3.16				
	X_2	W2			−0.99					−1.18				
	W1	W2			−4.17		**−7.61**			−4.13		**−8.47**		
	X_2	W1	W2		−8.74			**−1.30**		−10.11			**−1.18**	
				%		**1.84** R	87.02	14.82			**2.04R**	83.81	18.23	
2b						**0.06**					**0.07**			
	X_2	W1			−2.88					−3.72				
	X_2	W2			−2.88					−3.72				
	W1	W2			+0.56		**−5.71**			+0.05		**−7.40**		
	X_2	W1	W2		−4.98			**0.67**		−6.38			**0.94**	
				%			**1.26R**	114.67	13.45R			**1.07R**	115.84	14.78R
3a						**0.46**					**0.51**			
	X_2	W1			−0.42					−0.55				
	X_2	W2			−2.79					−3.61				
	X_2	W3			−0.01					0.02				
	W1	W2			−3.62					−3.52				
	W1	W3			−4.06					−4.04				
	W2	W3			−4.00		**−14.90**			−3.99	**−15.69**			
	X_2	W1	W2		−7.39	0.41	−6.83	−0.97		−8.56	0.47	−7.69	−1.34	
	X_2	W1	W3		−6.43	0.31	−6.80	0.05		−7.09	0.35	−7.57	0.13	
	X_2	W2	W3		−4.58	0.42	−4.49	−0.51		−4.68	0.23	−4.57	−0.34	
	W1	W2	W3		−14.09	0.42	−11.67	−2.83		−13.96	0.46	−11.55	−2.87	
	X_2	W1	W2	W3	−17.55			**−3.47**	0.37	−18.54			**−4.42**	1.07
3b						**0.47**					**0.63**			
	X_2	W1			−1.94					−2.85				
	X_2	W2			−0.20					−0.45				
	X_2	W3			−0.85					−0.97				
	W1	W2			−0.96					−3.88				
	W1	W3			−4.04					−1.27				
	W2	W3			−4.16		**−12.14**			−4.04		**−13.46**		
	X_2	W1	W2		−3.86	0.34	−3.09	−1.11		−5.97	0.38	−5.47	−0.89	
	X_2	W1	W3		−5.66	0.29	−5.21	−0.75		−9.68	0.61	−7.70	−2.59	
	X_2	W2	W3		−8.30	0.44	−6.83	−1.91		−5.32	0.49	−4.57	−1.24	
	W1	W2	W3		−10.36	0.33	−9.16	−1.53		−10.52	0.42	−9.18	−1.76	
	X_2	W1	W2	W3	−16.80			**−5.30**	0.18	−18.53			**−6.46**	0.76

[a] All energies are in kcal/mol and are BSSE corrected. Percent values correspond to the contribution of the many-body terms to the total interaction energy. *R* denotes a repulsive contribution.

sponding 1:1 complexes, especially the XH bound pair in **2a**. As expected, the difference in stability of this pair of structures comes from the HB present in **2a**, where 3-body contributions represent at least 15% of the total interaction energy. Furthermore, the relevance of strong HB for the stability of these structures also appears in the analysis of structure **2c**, where the distance between water molecules to form a HB is too large, 3.9 and 4.3 Å for Cl_2 and Br_2, respectively. Nonetheless, the arrangement of the three molecules in the plane favors a weak interaction between water molecules that conduces to a stabilizing three-body term.

None of these geometries match the stable structures found by Pathak et al.[34,41] for clusters of this size. Their minimum for Cl_2 has two hydrogen-bonded water molecules, but the second one is not pointing toward the halogen molecule; thus, no XH bond is formed. The structure they report for Br_2 results from adding a XB water molecule to structure **1c** (**1a** + **1c**) and is not a minimum at this level of calculation.

For the $X_2-(H_2O)_3$ clusters it is possible to observe the presence of several different types of XB and HB bonds. For both Cl_2 and Br_2, the most stable structure corresponds to the halogen making an XB to a cyclic water trimer, resulting in an almost perpendicular alignment, ∼93° to the trimer plane, while retaining the near tetrahedral H−O−X nearest neighbor angles. This result is not too surprising since the cyclic trimer structure is the global minimum on the water trimer PES[38,42−44] and since hydrogen bonding is stronger than XB bonding. Subtracting the water trimer bonding energy from that of structure **3a** shows that the XB bond energy is 15.4% (2.7 kcal/mol) for Cl_2 and 20.0% (3.7 kcal/mol) for Br_2. These values suggest that for this structure a single XB is formed between the water molecules and the halogen. This also reflects on the fact that the extent of charge transfer and polarization of the halogens is similar for structures **3a** and **1a**. The search of stable structures found several other true minima similar to **3a**. The main difference among them is not due to bonding to the other O atom lone pairs but is the angle X_2 forms with the plane that contains the three O atoms. In most cases, energy differences were smaller than 0.5 kcal/mol.

Structure **3b** can be thought of as resulting from one of the halogen atoms inserting into the water trimer ring. As for structure **2a**, both an XB and an XH bond are formed to a single halogen atom. This geometry results in a slightly less stable geometry, <1 kcal/mol, than **3a** for Cl_2 and almost isoenergetic for Br_2. Each of the heavy atoms lies in the same plane. That cooperative effects are important is revealed by the fact that both the XB and the XH distances are shorter than the analogous interactions for the 1:1 complexes. Cooperative effects are also reflected in the amount of charge transfer and polarization, which

are considerably larger than that of structure **3a** but also larger than **2a**, where both XB and XH interactions are present.

Structure **3c** is considerably less stable than **3a** and exhibits large X···O and X···H distances and a nonlinear Br−Br−O angle (∼120°). This is the only case in which we cannot confirm the presence of either a XB or a XH bond in the structure. Furthermore, the contribution of the halogen−water interaction to the overall stability of the clusters is less than 1 kcal/mol. Of the four studied structures for $X_2-(H_2O)_3$ clusters, **3d** is the one that has the closest resemblance to the structures found by Pathak et al.[34] The stability of this structure is less than the combined stabilities of structures **2a** and **1a** for both halogens.

For each of the $X_2-(H_2O)_3$ clusters the combined three-body terms are a stabilizing contribution to the total interaction energy. However, the effects vary between clusters. As expected, for structure **3a** (and for **3c**) the most important 3-body contribution is the one coming from the water trimer itself. The total three-body contribution accounts for ∼20−24% of the total interaction energy, and 80% of that term comes exclusively from the hydrogen-bonded water molecules. In contrast, for **3b** the three-body terms are 32% and 35% of the total E_{int} for Cl_2 and Br_2. There is not a single leading term, but cooperative effects are quite important as expected from the charge transfer and charge redistribution phenomena. The considerably smaller stability of structure **3d** is directly related to the small contribution of three-body terms to its stabilization.

Three stable clusters for the $X_2-(H_2O)_4$ system were located; in contrast to what was found for smaller clusters like **2a** and **3b**, all stable structures have molecular interactions that involve the two halogen atoms of the X_2 molecule. Similar to **3a**, and for the same reasons, the most stable geometry **4a** corresponds to a cyclic arrangement of the water molecules. As for $X_2-(H_2O)_3$ the most stable structure of $X_2-(H_2O)_4$ corresponds to the halogen forming a bond to one of the oxygen atoms of the water ring. However, for the larger system, the water cycle is able to bend to increase the interaction with the halogen molecule. The H atom pointing to the X_2 molecule is closer to the XB halogen atom than to the free one (3.301 vs 3.926 Å in Cl_2 and 3.319 vs 4.255 Å in Br_2). Still the angle is significantly smaller (∼110°) than those found for **1b** or **1c**. Thus, rather than a XH bond it is better to describe the H atom in the water molecule as interacting with the quadrupole of X_2. Moreover in this conformation the X_2 contribution to the total stability accounts for 12% and 17% for Cl_2 and Br_2, respectively, less than that found for structure **3a**.

The shortest XB interactions of this study were found in structure **4b**; they are 0.27 and 0.30 Å shorter than the corresponding X···O distances in structure **1a** and 0.21 and 0.45 Å shorter than the corresponding distances in structure **1b** for Cl_2 and Br_2, respectively. As for **3b**, there is a large charge transfer from the XB water molecule to the halogen, 0.05 for Cl_2 and 0.08 for Br_2. There is also an important charge delocalization through the cycle but not as large as for **3b** because of the presence of both halogen atoms in the chain and the lack of planarity in the cycle formed. In structure **4c** the possible number of molecular interactions is maximized, but this does not provide additional stability to the cluster since the polarization effects resulting of a motif such as **2a** are counterbalanced by the symmetry in this structure.

As for the smaller systems, the stability of the water cluster also determines the energetic hierarchy on the $X_2-(H_2O)_5$ clusters. The cyclic water structure is 1.8 kcal/mol more stable than the pyramidal structure.[45] However, when a X_2 molecule binds to the cyclic (**5a**) or the pyramidal structure (**5b**) this energy difference decreases significantly, 0.8 kcal/mol in the case of Cl_2 and 0.5 kcal/mol for Br_2. The optimal cyclic water structure is nonplanar (∼20°), and the presence of the halogen molecule enhances this bending by another ∼4−6°, resulting in enhanced stability compared to the smaller rings. Both the XB and the XH interaction distances are smaller than for the 1:1 complexes, in spite of not having the most favorable angular orientation. This reflects the fact that the halogen interactions only contribute 8.5% and 10.5% to the total interaction energy for Cl_2 and Br_2 clusters, respectively.

Structures **5b** and **5c** exhibit the H−quadrupole interaction previously described for structure **4a**. It is difficult to evaluate the net contribution of this interaction to the stability of these complexes. However, the fact that its presence results in lowering the energy difference between the cyclic and the pyramidal structure shows it makes a significant contribution to the overall stability.

The fact that our results do not coincide with those of Pathak et al.[34] motivated us to check if the differences were a consequence of the methodologies used. We performed some tests on bromine clusters using as starting geometries the same structures that led to the optimized MP2 structures shown above and performed DFT/B3LYP optimizations with the same basis set we selected for this work (aVDZ). For all the tested systems, $Br_2-(H_2O)_{2-4}$, we reached equivalent structures using the DFT method. Few, but significant, structural differences were found; Br···O distances tend to be slightly shorter (0.03−0.05 Å) and Br···H distances are significantly larger (0.10−0.30 Å) with DFT. In particular, for cyclic structures it was found that the halogen molecule does not lean over the cycle but points out of it. In all cases, the relative stabilities of the structures reported here are preserved using the DFT method. Further comparison between MP2- and DFT-optimized structures is beyond of the scope of this work.

As previous theoretical studies of halogen-bound systems have pointed out, the molecular interactions between halogens and water result in electric charge redistribution in the complex. Although X_2 molecules have no dipole moment, their quadrupole moment is large and modified because of the charge redistribution in the complex. Several works have studied this charge redistribution effect,[24,29,31,34,46,47] and charge differences between the halogen atoms larger than 0.10 au have been used to propose the presence of a charge-separated species in the clusters.[34] In this work, some of the effects arising from this charge redistribution phenomenon have already been discussed in terms of the charge transfer occurring through the XB. The Mulliken charge difference between the halogen atoms was calculated as a first approach to the charge distribution phenomena in these clusters, and then its validity was verified through the NBO analysis of charge distribution for some selected clusters. These two different methods lead to trends in good agreement, though the Mulliken analysis systematically predicts halogen polarization values ∼50% larger than does NBO. In Table 2 we present the X_2 polarization in each cluster. As expected, bromine is more polarized than chlorine: polarization effects range from 0.01 to 0.06 au for the former and from 0.06 to 0.10 au for the latter. It is interesting that the largest charge difference values are found in structures where a cycle in which the halogen and the water molecules participate is present, i. e., structures **2a**, **3b**, **4b**, **5a**, **5b**, and **5c**. We cannot confirm these cases correspond to charge-separated species, but it is clear that this partial ionicity in the halogens contributes to the strength of the interactions playing for these structures.

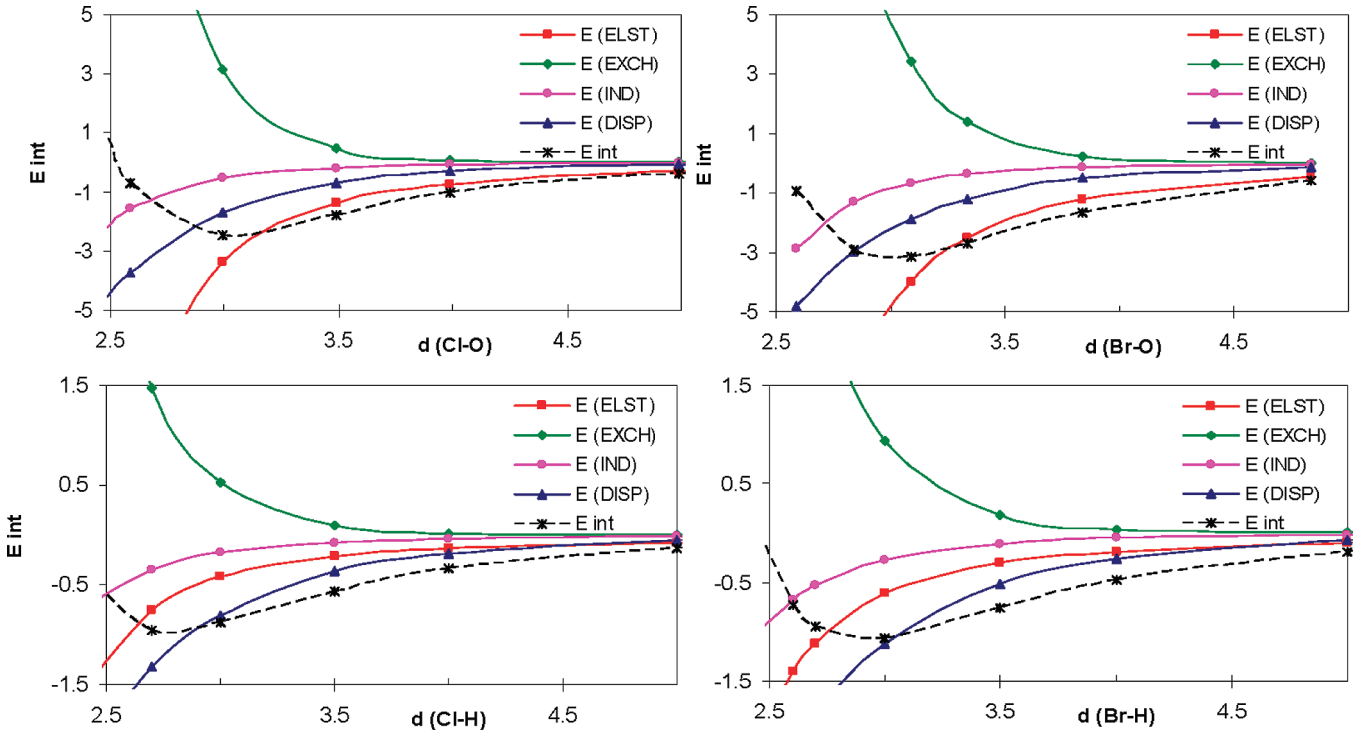

Figure 6. SAPT analysis of the terms contributing to the interaction energy of Cl_2-H_2O and Br_2-H_2O in two different configurations. The upper panel corresponds to the XB complexes, and the lower panel corresponds to the XH bound complexes. Distances are in Angstroms and interaction energies in kcal/mol.

B. SAPT Analysis of the X_2-H_2O Interaction. For these clusters, three bonding motifs are responsible of the structures found: hydrogen bonds, halogen bonds, and halogen−hydrogen interactions. For the hydrogen−halogen interactions we can further classify the bonds with respect to their angular orientation: XH bonding when only one halogen atom is involved, and H-quadrupole interaction when both halogen atoms are close to the H atom. To gain a deeper understanding of these interactions we calculated the different contributions to the interaction energy using the symmetry-adapted perturbation theory (SAPT). The interaction energy under the SAPT is the contribution of six first- and second-order terms,[48] $E_{int} = E^{(1)}_{pol} + E^{(1)}_{exch} + E^{(2)}_{ind} + E^{(2)}_{ex-ind} + E^{(2)}_{disp} + E^{(2)}_{ex-disp}$, that can be combined in the form of the physical recognizable interactions as the electrostatic term, $E_{ELST} = E^{(1)}_{pol}$, the induction term, $E_{IND} = E^{(2)}_{ind} + E^{(2)}_{ex-ind}$, the dispersion term, $E_{DISP} = E^{(2)}_{disp} + E^{(2)}_{ex-disp}$, and the exchange term, $E_{EXCH} = E^{(1)}_{exch}$.[49] In Figure 6 we present these contributions to the interaction energy on two of the monohydrated complexes studied, one of them with an XB (**1a**) and the other with a XH interaction (**1b**).

For each type of interaction between halogens and a water molecule, the electrostatic term dominates at long range and induction and dispersion forces are important in the minima region. Furthermore, the preferred angular orientations for the above-mentioned types of bonds can be rationalized based on having the dipole−quadrupole interaction dictate the relative orientation between the water molecules and the halogen and other terms (mainly induction) determining finer orientational details such as the XH bond vs the H−quadrupole interaction. However, the main difference between halogen (XB) and hydrogen-bound (XH) species is that for the former the electrostatic and induction terms are the leading contributions, whereas for the latter dispersion is the leading term. However, all terms are important for an accurate description. The fact that electrostatic and induction forces are weak for XH interactions explains why these bonds are not as strong as halogen bonds. The relative electrostatic, induction, and dispersion contributions to the stability of XB complexes are very similar for chlorine and bromine, with 60% of the total attractive contributions coming from the electrostatic term, 10% from the induction, and 30% from dispersion. For the XH-bound complexes, the relative contribution of the attractive terms for both halogens is identical: 31% from the electrostatic term, 14% from the induction, and 55% from the dispersion term.

II. Spectroscopic Properties of the $X_2-(H_2O)_n$ Clusters. The harmonic frequency analysis calculated for each structure can be used as a first approximation to the vibrational spectra of these systems. We will focus our analysis on two effects: the shift on the halogen stretching frequency upon cluster formation and the differentiation between the water molecules as a result of the specific intermolecular interactions they are engaged in. The shifts for the halogen molecule are presented in Table 4. The stretching mode for Cl_2 and Br_2 occurs in the far-IR region, and it overlaps some of the restricted translations or librational modes of the water molecules in the cluster. For this reason it is quite common, particularly for bromine, that the stretching mode is coupled with the intermolecular stretching and torsion modes. The large red shifts for both halogens are due to strong halogen bonding. However, this shift is considerably larger for structures **3b** and **4b** as a consequence of the charge transfer to the X_2 molecule. This difference may be useful to correctly identify the coordination motifs present in gas-phase experiments. However, the coincidence of this band with the librational modes of the water molecules might impede a proper detection of this shift. Resonance Raman spectroscopy could be used to distinguish between the halogen stretch and other nearby modes.

The mid-IR region of the spectra, containing the stretching signature of the OH bonds in the complexes, might prove to be extremely useful for identification purposes as has been the case

TABLE 4: Calculated Shifts for the Halogen−Halogen Stretching Band[a]

cluster	structure	Δν, X = Cl	Δν, X = Br
X_2-H_2O	**1a**	−17	−10
	1b	0	0
	1c	0	0
$X_2-(H_2O)_2$	**2a**	−29	−19
	2b	−25	−13
	2c	−18	−10
$X_2-(H_2O)_3$	**3a**	−22	−11[b]
	3b	−40	−29
	3c	0	0
	3d	−31	−17[b]
$X_2-(H_2O)_4$	**4a**	−20[b]	−16[b]
	4b	−61[b]	−41[b]
	4c	−38	−24[b]
$X_2-(H_2O)_5$	**5a**	−16	−18[b]
	5b	−22	−16[b]
	5c	−23	−13[b]

[a] $\Delta\nu = \nu_{X2complex} - \nu_{x2}$ in cm^{-1}. For Cl_2 at this level ν = 537.7 cm^{-1}, and for Br_2 ν = 313.5 cm^{-1}. [b] Additional normal modes with X−X stretching were found coupled with water vibrations. See text.

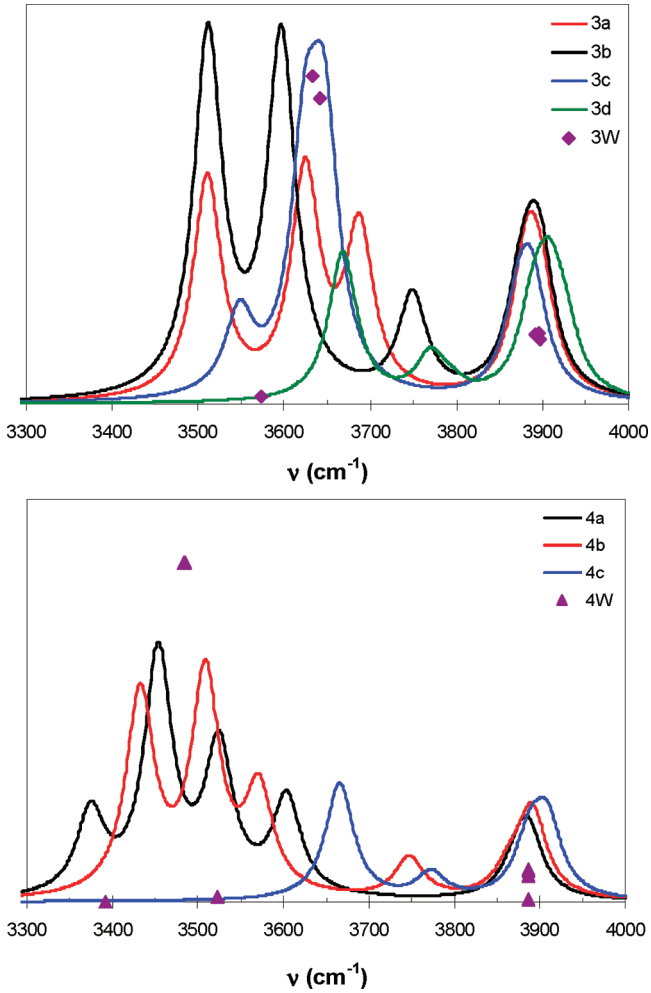

Figure 7. Part of the simulated IR spectra for the harmonic vibrational analysis of the $Cl_2-(H_2O)_3$ and $Cl_2-(H_2O)_4$ clusters. Solid points correspond to the frequencies and intensities of the cyclic water trimer and tetramer as reported in ref 42.

for other hydrogen-bonded clusters.[50−53] In Figure 7 the simulated vibrational spectra for $Cl_2-(H_2O)_3$ and $Cl_2-(H_2O)_4$ are shown. For comparison, the vibrational frequencies and intensities for the cyclic water trimer and tetramer are also

TABLE 5: Calculated Shifts for the $B(^3\Pi_u) \Leftarrow X$ Electronic Transition of the Halogen Molecule in the $X_2-(H_2O)_n$ Clusters[a]

		X = Cl		X = Br	
cluster	structure	δν (MP2)	δν (CCSD(T))	δν (MP2)	δν (CCSD(T))
X_2-H_2O	**1a**	1461	1383	2054	1983
	1b	621	493	624	533
	1c	615	488	640	571
$X_2-(H_2O)_2$	**2a**	1752	1689	2892	2724
	2b	2606	2516	3626	3471
	2c	1565	1497	2220	2154
$X_2-(H_2O)_3$	**3a**	1544	1504	2372	2294
	3b	2089	2003	6739	4465
	3c	950	159	633	68
	3d	2925	2823	4157	4018
$X_2-(H_2O)_4$	**4a**	1449	1347	2186	2123
	4b	3388	2305	5944	5011
	4c	3904	3785	5636	5231
$X_2-(H_2O)_5$	**5a**	2789	1837	3150	2588
	5b	1934	1854	5214	3069
	5c	2369	2124	3608	3319

[a] All values (cm^{-1}) were obtained as $\delta\nu = T_v(X_2-(H_2O)_n) - T_v(X_2)$.

shown. The O−H stretching motions are conveniently defined as bonded O−H stretches for those participating in hydrogen bonds between water molecules and dangling or free O−H stretches. As expected, the bonded stretches are significantly red shifted relative to the stretching modes of isolated water and appear in the 3300−3700 cm^{-1} region, whereas the dangling stretches appear in the neighborhood of 3900 cm^{-1}, slightly red shifted from the asymmetric stretching frequency in water. The region of the spectra corresponding to the bonded stretches is quite sensitive to the coordination patterns present in the clusters, but the region corresponding to the free stretches is not. This analysis shows that for the molecules taking part in XB the bond stretch bands are slightly blue shifted with respect to those only participating in HB. On the other hand, the band appearing at ∼3740 cm^{-1} is indicative of a strong XH bond and will certainly allow the definitive identification of structures **3b** and **4b** if they appear in gas-phase experiments.

We also calculated the expected electronic shifts for the transition to the lowest triplet state that correlates with the well-known B $^3\Pi_u$ state of the halogen. The shift is obtained as the difference in the vertical excitation energies (T_v) in the complex and for the isolated halogen. In Table 5 we present the results obtained when using the RMP2 and RCCSD(T) methods together with the aug-cc-pVDZ basis. As discussed in our previous study[27] the large blue shift for the XB interaction is due to the attractive interaction in the ground state of the complex plus the repulsive interaction in the excited state. The repulsive interaction in the excited state originates both from a change of sign in the halogen quadrupole moment and from a substantial increase in the exchange−repulsion between the monomers due to the $\pi^* \Rightarrow \sigma^*$ electron excitation involved in the electronic transition.

For the XH interaction, the blue shift is significantly smaller as seen from the values reported for structures **1b** and **1c** since there is little exchange−repulsion in this case. A quick glance at the table shows a large variation in the shift values as a function of the size and geometry of the cluster. A rough understanding of these variations can be obtained by estimating the shift based on pairwise additive counting of the XB and XH interactions present in a given cluster. This procedure works

well when the O−X and H--X distances in the species studied are similar to those in the corresponding 1:1 complexes (structures **1a**−**c**). When the distances become shorter, the shifts can be much larger, and this can still be qualitatively understood based on a larger contribution arising from the repulsive interaction in the excited state. For example, if we look at the shifts for structures **2a**−**c** we predict **2b** to have the largest shift and approximately be equal to twice the shift for a regular XB. Analogously, we would predict similar shifts for structures **2a** and **2c**, which is approximately true. The fact that **2a** has larger shifts than **2c** can be rationalized from the fact that the O−X distance is shorter in the former. Obviously, the use of this model is only qualitative since clearly a quantitative determination depends on many-body effects, which may be different in the ground and excited electronic states.

Regarding the performance of RMP2 vs RCCSD(T) we see that, in general, it reproduces the correct ordering of the shifts for the different structures, and for many cases the absolute values are within 10% of each other. This will make RMP2 a valuable tool for estimating shifts in larger clusters. Still there are some cases in which RMP2 deviates significantly from RCCSD(T): notably, structures **3c**, **5a**, and **5b**. The problem is that RMP2 cannot recover the high-order correlation necessary to describe weak interactions characterizing the excited state. In other cases, i.e., structure **4b**, the interplay of several factors such as charge polarization and weak interactions requires a high-level treatment even for quantitative estimates.

Discussion

In this study, several aspects of the intermolecular interactions responsible for the stability of $X_2-(H_2O)_n$ clusters were considered. The coexistence of hydrogen bonds, halogen bonds, and a third type of interaction halogen−hydrogen bond allowed us to analyze the interplay between them and their similarities and differences that result in a wide variety of interesting structures with differing contributions of the several types of intermolecular forces.

It is interesting to compare the halogen bonds studied here to the more general case of a single halogen atom bonded to carbon and interacting with electron-donating species. The SAPT analysis was recently applied to several examples by Riley and Hobza.[49] They found that the dispersion interaction was the leading term for the complexes they studied. In contrast, for the X−X···O bonds studied here electrostatic and induction contributions are more important, similar to the case of normal hydrogen bonding. This difference may be important for evaluating the magnitude of the forces acting on larger systems such as protein−ligand complexes or composite materials.

For the XB formed in $X_2-(H_2O)_n$ clusters it was found that the shorter X···O distances (**4b** < **3b** < **2a** < **1a**) correlate with the longer X−X distances (**1a** < **2a** < **3b** < **4b**) and smaller halogen stretching vibrational frequencies. This shorter XB bond and longer X−X bond also occur for the structures in which a second donating group coordinates to the X−X molecule, but the effect is somewhat smaller. The linearity of the X−X···O interaction was confirmed in all the studied systems.

Although XB bonding is the most important water−halogen interaction in the clusters studied here, X−H bonding leads to local minima in smaller clusters, **1b**, **1c**, **2a**, and **2c**, and plays an important role in all of the larger clusters. However, not all XH interactions are equivalent. Some of them can be understood in terms of a favorable electrostatic interaction between the H^+ and the polarized π and π^* densities in the nearest X atom. In contrast, for cyclic structures it was found that the hydrogen atom pointed to the center of the X−X moiety. This case is more consistently described as a result of the large quadrupole moment of X_2. It resembles the interaction between water and the π bond in ethylene.[54] For both the XH bond and the X−quadrupole bonds dispersion plays an important role; it is clear that this interaction must not be considered as a particular type of hydrogen bond. The large dispersion contribution to XH interactions also helps to explain the differences observed in the structures obtained using DFT methodologies and those reported here.

The XH interaction for structures **2a** and **3b** is somewhat different from the two cases discussed in the previous paragraph because it occurs between two positively charged atoms.[39] ($X^{\delta+}(\sim 0.05)\cdots{}^{\delta+}(\sim 0.20)H$). Also, in contrast with most H bonds and X bonds the geometry is not linear (∼125−160°). In this case, one can expect that models based on point charges will fail, and it will be important to include each of the contributing factors, i.e., the dipole−quadrupole interaction, induction or polarization of the π and π^* densities, and, of course, dispersion.[31,40]

As expected, interaction energies are larger for the clusters containing bromine than for the ones containing chlorine. However, these differences decrease as the cluster size increases. Br_2 has a larger quadrupole moment and is more polarizable than Cl_2, leading to larger induction and polarization effects that also result in larger three-body stabilization contributions. Also, charge transfer is more important for Br_2 than for Cl_2. Furthermore, the total contribution of the X_2−water interaction to the total stability of the clusters containing a cyclic water cluster motif (**3a**, **4a**, and **5a**) decreases as the size of the water ring grows even though the charge transfer to X_2 grows. Since the differences between Cl_2 and Br_2 are less significant for the larger clusters one might have also expected small differences for condensed phase phenomena. However, as noted in the introduction, the blue shift between the gas phase and aqueous solution is considerably larger for valence excitation spectra of bromine, 1750 cm^{-1}, than for chlorine, 550 cm^{-1}.

It is also important to note that the calculated shifts for the absorption spectra for most of these clusters studied here are larger than the experimentally measured shifts for Cl_2 and Br_2 in aqueous solution. Isomers of similar stability can have very different electronic shifts. In liquid solution the electronic spectra show a broadening of the bands compared with the gas phase. One possible explanation for this broadening could be that they reflect the fluctuations in the structure of the solvation shell surrounding the halogen. The theoretical calculation of the observed shifts and broadening of the spectra will require the simulation of the statistical distribution of solute−solvent configurations which is more complicated than the restricted minimum energy configurations studied here.

Conclusions

The structures of the $X_2-(H_2O)_n$ clusters depend on a subtle interplay of hydrogen, halogen, and XH bonding and thus also between the electrostatic, induction, and dispersion forces. Many-body effects are also quite important. Are they competing or complementary forces? The analysis of the most stable structures confirms that halogen bonding enhances hydrogen bonding: structures **2a**, **3b**, and **4b** are definitely good examples of this synergy. In particular, formation of a halogen bond enhances the three-body interaction for hydrogen bonding in cases that include cyclic water subclusters. Although the XH interaction is less strong than either hydrogen bonding or

halogen bonding, it plays an important role in determining the stable structures for larger clusters. Its presence conveys greater stability to the aggregate through significant cooperative effects.

The vibrational shifts and spectra calculated in this work indicate it should be possible to identify many of the isomeric structures in IR and/or Raman studies of the clusters. Similarly, the electronic shifts vary substantially between isomers, and this should be reflected in their experimental electronic spectra. Although the calculated shifts for the clusters studied in this paper offer insight for the interpretation of condensed phase spectra, it is clear that much still needs to be done before a qualitative and quantitative explanation can be given. A suitable model for studying halogen solvation and associated spectroscopy must be able to reproduce the subtle interplay between all of the possible interactions present in these systems in both the ground and the excited electronic states.

Acknowledgment. This paper is dedicated to Prof. Iván Ortega-Blake on the occasion of his birthday. We thank the collaboration of J. Alfredo González Espinoza and the valuable discussions with Galina Kerenskaya. This project was supported by NSF-CONACYT J110.385, CONACYT 79975, and the NSF grant CHE-0404743. M.I.B.U. is currently an UCMEXUS-CONACYT Sabbatical Fellow at UCI.

Supporting Information Available: Many body analysis for the $X_2-(H_2O)_2$ and $X_2-(H_2O)_3$ clusters. This information is available free of charge via the Internet at http://pubs.acs.org

References and Notes

(1) Kerenskaya, G.; Goldschleger, I. U.; Apkarian, V. A.; Fleischer, E.; Janda, K. C. *J. Phys. Chem. A* **2007**, *111*, 10969.
(2) Kerenskaya, G.; Goldschleger, I. U.; Apkarian, V. A.; Janda, K. C. *J. Phys. Chem. A* **2006**, *110*, 13792.
(3) Janda, K. C.; Kerenskaya, G.; Goldschleger, I. U.; Apkarian, V. A.; Fleischer, E. UV-Visible and Resonance Raman Spectroscopy of Halogen Molecules in Clathrate-Hydrates. *Proceedings of the 6th International Conference on Gas Hydrates (ICGH 2008)*; Vancouver, British Columbia, Canada, 2008; https://circle.ubc.ca/bitstream/2429/1476/1/5393.pdf.
(4) Bayliss, N. S.; Cole, A. R. H.; Green, B. G.; Aust, J. *Sci. Res. Ser. A: Phys. Sci.* **1948**, *1*, 472.
(5) Bayliss, N. S. *J. Chem. Phys.* **1950**, *18*, 292.
(6) Buckles, R. E.; Mills, J. F. *J. Am. Chem. Soc.* **1953**, *75*, 552.
(7) Bayliss, N. S.; Rees, A. L. G. *J. Chem. Phys.* **1939**, *7*, 854.
(8) Geilhaupt, M.; Dorfmuller, T. *Chem. Phys.* **1983**, *76*, 443.
(9) Renger, T.; Grundkötter, B.; Madjet, M. E.-A.; Müh, F. *Proc. Natl. Acad. Sci.* **2008**, *105*, 13235.
(10) Harris, S. J.; Novick, S. E.; Klemperer, W.; Falconer, W. E. *J. Chem. Phys.* **1974**, *61*, 193.
(11) Kubiak, G.; Fitch, P. S. H.; Wharton, L.; Levy, D. H. *J. Chem. Phys.* **1978**, *68*, 4477.
(12) Evard, D. D.; Cline, J. I.; Janda, K. C. *J. Chem. Phys.* **1988**, *88*, 5433.
(13) Evard, D. D.; Bieler, C. R.; Cline, J. I.; Sivakumar, N.; Janda, K. C. *J. Chem. Phys.* **1988**, *89*, 2829.
(14) Halberstadt, N.; Beswick, A.; Roncero, O.; Janda, K. C. *J. Chem. Phys.* **1992**, *96*, 2404.
(15) Burke, M. L.; Klemperer, W. *J. Chem. Phys.* **1993**, *98*, 6642.
(16) Rohrbacher, A.; Williams, J.; Janda, K. C. *Phys. Chem. Chem. Phys.* **1999**, *1*, 5263.
(17) Rohrbacher, A.; Halberstadt, N.; Janda, K. C. *Annu. Rev. Phys. Chem.* **2000**, *51*, 405.
(18) Cabrera, J.; Bieler, C. R.; McKinney, N.; Veer, W. E. v. d.; Pio, J. M.; Janda, K.; Roncero, O. *J. Chem. Phys.* **2007**, *127*, 164309.
(19) Pio, J. M.; van der Veer, W. E.; Bieler, C. R.; Janda, K. C. *J. Chem. Phys.* **2008**, *128*, 134311.
(20) Burke, M. L.; Klemperer, W. *J. Chem. Phys.* **1993**, *98*, 1797.
(21) Darr, J. P.; Glennon, J. J.; Loomis, R. A. *J. Chem. Phys.* **2005**, *122*, 131101.
(22) Legon, A. C. *Angew. Chem., Int. Ed.* **1999**, *38*, 2686.
(23) Legon, A. C.; Thumwood, J. M. A. *Phys. Chem. Chem. Phys.* **2001**, *3*, 2758.
(24) Legon, A. C.; Thumwood, J. M. A.; Waclawik, E. R. *Chem.—Eur. J.* **2002**, *8*, 940.
(25) Davey, J. B.; Legon, A. C.; Thumwood, J. M. A. *J. Chem. Phys.* **2001**, *114*, 6190.
(26) Davey, J. B.; Legon, A. C. *Phys. Chem. Chem. Phys.* **2001**, *3*, 3006.
(27) Hernández-Lamoneda, R.; Uc-Rosas, V. H.; Bernal-Uruchurtu, M. I.; Halberstadt, N.; Janda, K. C. *J. Phys. Chem. A* **2008**, *112*, 89.
(28) Goldschleger, I. U.; Kerenskaya, G.; Janda, K. C.; Apkarian, V. A. *J. Phys. Chem. A* **2008**, *112*, 787.
(29) Legon, A. C. The interaction of dihalogens and hydrogen halides with Lewis bases in the gas phase: An experimental comparison of the halogen bond and the hydrogen bond. In *Halogen Bonding: Fundamentals and Applications*; Springer-Verlag: Berlin, Heidelberg, 2008; Vol. 126, p 17.
(30) Clark, T.; Hennemann, M.; Murray, J.; Politzer, P. *J. Mol. Model.* **2007**, *13*, 291.
(31) Politzer, P.; Lane, P.; Concha, M.; Ma, Y.; Murray, J. *J. Mol. Model.* **2007**, *13*, 305.
(32) Politzer, P.; Murray, J. S.; Lane, P. *Int. J. Quantum Chem.* **2007**, *107*, 3046.
(33) Murray, J. S.; Lane, P.; Politzer, P. *Int J. Quantum Chem.* **2007**, *107*, 2286.
(34) Pathak, A. K.; Mukherjee, T.; Maity, D. K. *J. Phys. Chem. A* **2008**, *112*, 744.
(35) Frisch, M. J.; Trucks, G. W.; Schlegel, H. B; Scuseria, G. E.; Robb, M. A.; Cheeseman, J. R.; Zakrzewski, V. G.; Montgomery, J. A., Jr.; Stratmann, R. E; Burant, J. C.; Dapprich, S.; Millam, J. M.; Daniels, A. D.; Kudin, K. N.; Strain, M. C.; Farkas, O.; Tomasi, J.; Barone, V.; Cossi, M.; Cammi, R.; Mennucci, B.; Pomelli, C.; Adamo, C.; Clifford, S.; Ochterski, J.; Petersson, G. A.; Ayala, P. Y.; Cui, Q.; Morokuma, K.; Rega, N.; Salvador, P.; Dannenberg, J. J.; Malick, D. K.; Rabuck, A. D.; Raghavachari, K.; Foresman, J. B.; Cioslowski, J.; Ortiz, J. V.; Baboul, A. G.; Stefanov, B. B.; Liu, G.; Liashenko, A.; Piskorz, P.; Komaromi, I.; Gomperts, R.; Martin, R. L.; Fox, D. J.; Keith, T.; Al-Laham, M. A.; Peng, C. Y.; Nanayakkara, A.; Challacombe, M.; Gill, P. M. W.; Johnson, B.; Chen, W.; Wong, M. W.; Andres, J. L.; Gonzalez, C.; Head-Gordon, M.; Replogle, E. S.; Pople, J. A. *Gaussian*, Revision A.11.3 ed.; Gaussian, Inc.: Pittsburgh, PA, 2002.
(36) Werner, H.-J.; Knowles, P. J.; Amos, R. D.; Bernhardsson, A.; Berning, A.; Celani, P.; Cooper, D. L.; Deegan, M. J. O.; Dobbyn, A. J.; Eckert, F.; Hampel, C.; Hetzer, G.; Korona, T.; Lindh, R.; Lloyd, A. W.; McNicholas, S. J.; Manby, F. R.; Meyer, W.; Mura, M. E.; Nicklass, A.; Palmieri, P.; Pitzer, R.; Rauhut, G.; Schutz, M.; Schumann, U.; Stoll, H.; Stone, A. J.; Tarroni, R.; Thorsteinsson, T.; Leininger, M. L. *Molpro*, version 2004.1, a package of ab initio programs; see http://www.molpro.net.
(37) Pastor, N.; Ortega-Blake, I. *J. Chem. Phys.* **1993**, *99*, 7899.
(38) Xantheas, S. *Chem. Phys.* **2000**, *258*, 225.
(39) Wang, F. F.; Hou, J. H.; Li, Z. R.; Wu, D.; Li, Y.; Lu, Z. Y.; Cao, W. L. *J. Chem. Phys.* **2007**, 126.
(40) Politzer, P.; Murray, J. S.; Concha, M. C. *J. Mol. Model.* **2008**, *14*, 659.
(41) Pathak, A. K.; Mukherjee, T.; Maity, D. K. *J. Chem. Phys.* **2006**, *124*, 024322.
(42) Xantheas, S.; Dunning, T. H. J. *J. Chem. Phys.* **1993**, *99*, 8744.
(43) Xantheas, S. S. *J. Chem. Phys.* **1994**, *100*, 7523.
(44) Keutsch, F. N.; Cruzan, J. D.; Saykally, R. J. *Chem. Rev.* **2003**, *103*, 2533.
(45) Hodges, M. P.; Stone, A. J.; Xantheas, S. S. *J. Phys. Chem. A* **1997**, *101*, 9163.
(46) Alkorta, I.; Rozas, I.; Elguero, J. *J. Phys. Chem. A* **1998**, *102*, 9278.
(47) Davey, J. B.; Legon, A. C.; Thumwood, J. M. A. *J. Chem. Phys.* **2001**, *114*, 6190.
(48) Jeziorski, B.; Moszynski, R.; Szalewicz, K. *Chem. Rev.* **1994**, *94*, 1887.
(49) Riley, K. E.; Hobza, P. *J. Chem. Theory Comput.* **2008**, *4*, 232.
(50) Zou, J.-W.; Jiang, Y.-J.; Guo, M.; Hu, G.-X.; Zhang, B.; Liu, H.-C.; Yu, Q.-S. *Chem.—Eur. J.* **2005**, *11*, 740.
(51) Groenenboom, G. C.; Wormer, P. E. S.; van der Avoird, A.; Mas, E. M.; Bukowski, R.; Szalewicz, K. *J. Chem. Phys.* **2000**, *113*, 6702.
(52) Steinbach, C.; Andersson, P.; Melzer, M.; Kazimirski, J. K.; Buck, U.; Buch, V. *Phys. Chem. Chem. Phys.* **2004**, *6*, 3320.
(53) Jiang, J.-C.; Wang, Y.-S.; Chang, H.-C.; Lin, S. H.; Lee, Y. T.; Niedner-Schatteburg, G.; Chang, H.-C. *J. Am. Chem. Soc.* **2000**, *122*, 1398.
(54) Tarakeshwar, P.; Kim, K. S. *J. Mol. Struct.* **2002**, *615*, 227.

JP900490P